Insertion Loss of Electronically Variable Magnetostatic Wave Delay Lines

S. N. BAJPAI, SENIOR MEMBER, IEEE

Abstract—**This paper presents an investigation of insertion loss and constant variable delays in electronically variable magnetostatic volume wave delay lines. The delay line has a conductor–dielectric–YIG–dielectric–conductor structure. Variable delays up to 300 MHz have been obtained in single volume wave delay line by adjusting the direction and magnitude of the biasing dc magnetic field in a plane containing the normal to the YIG film and the direction of wave propagation. Insertion loss as a function of frequency has been obtained for different biasing field angles and also for the angles corresponding to variable constant delays. Comparison of theoretically obtained insertion loss has been made with experimental results, and good agreement is found. Electronically variable magnetostatic wave delay lines have promising applications in broad-band phased array antennas at 1–20 GHz frequencies.**

I. INTRODUCTION

IT HAS BEEN demonstrated by continuous research and development efforts in the last two decades that magnetostatic waves (MSW's) have a great deal of potential in several devices, among them nondispersive, dispersive, and variable delay lines, bandpass filters, resonators, oscillators, signal-to-noise enhancers, convolvers, and filter banks [1]–[7]. Magnetostatic wave technology is based on the low-loss propagation of magnetostatic waves in biased yttrium iron garnet (YIG) thin films. The films are grown epitaxially on gadolinium gallium garnet substrates. Propagation loss as low as 20 dB/μs at microwave frequencies has been observed [1]. Magnetostatic waves are efficiently excited by simple microstrip transducers. The initial theory and experiment on the excitation were presented by Ganguly and Webb [8]. Later, several useful papers on the excitation of magnetostatic waves [9]–[15] were published. The alluring feature of MSW technology is the larger operating bandwidth directly (without the need for down-conversion of frequencies) at microwave frequencies. In addition to this, the dispersion and delay characteristics of MSW's can be tuned by varying the biasing dc magnetic field. It has been demonstrated in the past that MSW devices have enormous potential in modern communication and radar systems, where the signal can be processed directly at microwave frequencies.

Electronically variable delay lines have significant potential applications in broad-band phased array antennas. The first variable delays were demonstrated by Sethares *et al.* [16]. This was achieved through the use of two separate delay lines on "up-chirp" and "down-chirp" delay lines in cascade. Later, improved constant delay over a 250 MHz band variable by 20 percent was shown [17]. However the device has 35 dB insertion loss, across the band. This insertion loss, which is too high, is due to cascading of two delay lines. In a recent paper greatly improved results on the above device have been published [18]. The results are impressive; however loss is still high.

Another technique to achieve variable delay has been demonstrated by Bajpai *et al.* [19], where the constant delay over a 150 MHz frequency band variable by ± 20 percent was demonstrated in a single delay line. This was achieved by adjusting the direction and the magnitude of the applied magnetic field in the forward to backward volume wave plane. The insertion loss across the 150 MHz frequency band was measured to be approximately 15 dB. The study was later extended and it was shown that the bandwidth of variable delay can be enhanced by adding a second ground plane, and a bandwidth of 300 MHz was theoretically obtained [20].

This paper presents a study of variable constant delay and of insertion loss of variable magnetostatic delay line having a conductor–dielectric–YIG–dielectric–conductor configuration. The insertion loss and delay expressions have been obtained for the case where the internal magnetic field lies in the plane which contains the normal to the YIG film and the direction of propagation of the MSW (forward–backward volume plane). The variation of insertion loss with frequency has been obtained for certain biasing field directions. Nondispersive (constant) delays have been obtained and have been shown to be variable by adjusting the magnitude and the direction of the biasing magnetic field. The corresponding insertion loss with frequencies has also been shown. Finally, a comparison of insertion loss theoretically obtained has been made with the experimental results.

II. THEORY

The delay line structure is shown in Fig. 1. It consists of conductor–dielectric (Al_2O_3)–YIG–dielectric (GGG)–conductor. A magnetic field is applied in the $Z-X$ plane (forward–backward volume wave plane) and is rotated away relative to the Z axis. This arrangement excites

Manuscript received November 2, 1988; revised April 24, 1989. This work was supported by the National Science Foundation under Grant ECS-8504606.

The author is with the Department of Electrical Engineering, State University of New York, Stony Brook, NY 11794-2350.

IEEE Log Number 8929902.

0018-9480/89/1000-1529$01.00 ©1989 IEEE

magnetostatic forward and backward volume waves. The waves propagate in the x direction. Microwave current flows in single microstrips, which are used to excite and receive magnetostatic volume waves. For the case where the biasing dc field (internal magnetic field) is in a direction which makes an angle θ with the z axis, the relative permeability tensor has been obtained as [19]

$$\mu_r = \begin{bmatrix} \mu_{11} & \mu_{12} & \mu_{13} \\ \mu_{21} & \mu_{22} & \mu_{23} \\ \mu_{31} & \mu_{32} & \mu_{33} \end{bmatrix} \tag{1}$$

where

$$\mu_{11} = \mu\cos^2\theta + \sin^2\theta$$
$$\mu_{12} = jK\cos\theta$$
$$\mu_{13} = \sin(\theta)\cos(\theta)(1-\mu)$$
$$\mu_{21} = -jK\cos\theta$$
$$\mu_{22} = \mu$$
$$\mu_{23} = jK\sin\theta$$
$$\mu_{31} = (1-\mu)\sin(\theta)\cos\theta$$
$$\mu_{32} = -jK\sin\theta$$
$$\mu_{33} = \mu\sin^2\theta + \cos^2\theta.$$

Permeability tensor elements for the general direction of biasing magnetic field have previously been derived and are given in [19]. Equations (1) and (2) in this paper are obtained from [19] for the specific case where the biasing magnetic field lies in the plane which contains the normal to the YIG film and the direction of MSW propagation (or forward to backward volume wave plane). In (2), μ and K have been defined as

$$\mu = \frac{\omega_0(\omega_0+\omega_m)-\omega^2}{\omega_0^2-\omega^2} \qquad K = \frac{\omega\omega_m}{\omega_0^2-\omega^2}$$

and

$$\omega_0 = \gamma H \qquad \omega_m = \gamma 4\pi M_0 \tag{2}$$

where H, $4\pi M_0$, γ, and ω are the biasing dc magnetic field (internal dc magnetic field), the saturation magnetization, the gyromagnetic ratio, and the wave frequency, respectively. Under magnetostatic approximation, Maxwell's equations are written as

$$\nabla \times \boldsymbol{h} = 0 \qquad \nabla\cdot\boldsymbol{b} = 0$$

where wave magnetic induction $\boldsymbol{b}$ is written as $\boldsymbol{b} = \mu_0\mu_r\boldsymbol{h}$, μ_0 is the permeability of free space, and $\boldsymbol{h} = \nabla\psi$, ψ being the magnetic potential. It is assumed that the fields are uniform along the y direction. It is a good assumption for YIG films having widths of 5 mm and more. It has been shown [13] that the width modes propagating along the width of the YIG film are weakly excited and therefore that fields along the width or y direction can be assumed to be uniform. Magnetic potentials (ignoring

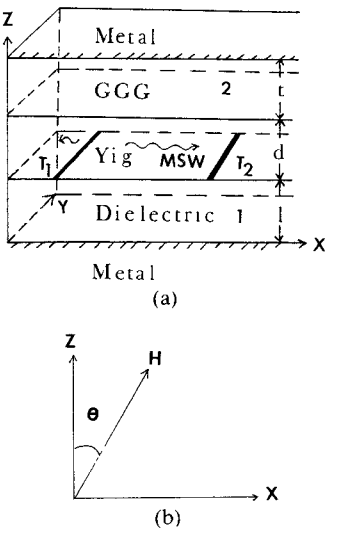

Fig. 1. (a) Magnetostatic volume wave delay line: l = thickness of region 1, d = thickness YIG, t = thickness of region 2, T_1 and T_2 are the exciting and receiving transducers respectively. (b) Direction of internal biasing magnetic field H with Z axis.

time dependence) in different regions are expressed as

$$\psi^{(1)} = \int_{-\infty}^{+\infty}[B_1\exp(\beta z) + B_2\exp(-\beta z)]\exp(-j\beta sx)\,d\beta$$

$$\psi^{\mathrm{YIG}} = \int_{-\infty}^{+\infty}\left[A_1\exp\left\{j\beta\left(p_0 s + \sqrt{p_0^2-n_0^2}\right)z\right\} + A_2\exp\left\{-j\beta\sqrt{p_0^2-n_0^2} - sp_0\right)z\right\}\right] \cdot\exp(-j\beta sx)\,d\beta$$

$$\psi^{(2)} = \int_{-\infty}^{+\infty}[C_1\exp(\beta z) + C_2\exp(-\beta z)]\exp(-j\beta sx)\,d\beta. \tag{3}$$

In (3) B_1, B_2, A_1, A_2, C_1, and C_2 are arbitrary constants which are evaluated by applying boundary conditions at the interfaces, s is positive for $+x$ excitation and $s=-1$ for $-x$ excitation, and β is the wavenumber of the magnetostatic wave. The functions $\psi^{(1)}$, ψ^{YIG}, and $\psi^{(2)}$ represent magnetic potentials in dielectric 1 (Al_2O_3), in YIG, and in dielectric 2 (GGG), respectively, and p_0 and h_0 are defined as

$$p_0 = \frac{(1-\mu)\sin\theta\cos\theta}{\mu_{33}} \tag{4}$$

$$n_0 = \left[\frac{\mu_{11}}{\mu_{33}}\right]^{1/2} = \left[\frac{\mu\cos^2\theta+\sin^2\theta}{\mu\sin^2\theta+\cos^2\theta}\right]^{1/2}. \tag{5}$$

The normal components of wave magnetic induction (b_z's) and the tangential components of magnetic field

(h_x's) in different regions are obtained from (3) as

$$b_z^{(1)} = \mu_0 \int_{-\infty}^{+\infty} \beta [B_1 \exp(\beta z) - B_2 \exp(-\beta z)] \exp(-j\beta s x)\, d\beta$$

$$b_z^{\mathrm{YIG}} = \mu_0 \int_{-\infty}^{+\infty} \Big[j\beta A_1 \Big\{ \mu_{33}\Big(sp_0 + \sqrt{p_0^2 - n_0^2}\Big) - s\mu_{31} \Big\} \cdot \exp\Big\{ j\beta \Big(sp_0 + \sqrt{p_0^2 - n_0^2}\Big) z \Big\} + j\beta A_2 \Big\{ \mu_{33}\Big(sp_0 - \sqrt{p_0^2 - n_0^2}\Big) - s\mu_{31} \Big\} \cdot \exp\Big\{ -j\beta \Big(\sqrt{p_0^2 - n_0^2} - sp_0\Big) z \Big\} \Big] \exp(-j\beta s x)\, d\beta$$

$$b_z^{(2)} = \mu_0 \int_{-\infty}^{+\infty} \beta [C_1 \exp(\beta z) - C_2 \exp(-\beta z)] \exp(-j\beta s x)\, d\beta. \quad (6)$$

In similar fashion, the h_x's $= \partial\psi/\partial x$ are obtained as

$$h_x^{(1)} = -js \int_{-\infty}^{+\infty} \beta [B_1 \exp(\beta z) + B_2 \cdot \exp(-\beta z)] \exp(-j\beta s x)\, d\beta$$

$$h_x^{YIG} = -js \int_{-\infty}^{+\infty} \beta \Big[A_1 \exp\Big\{ j\beta \Big(sp_0 + \sqrt{p_0^2 - n_0^2}\Big) z \Big\} + A_2 \exp\Big\{ -j\beta \Big(\sqrt{p_0^2 - n_0^2} - sp_0\Big) z \Big\} \Big] \cdot \exp(-j\beta s x)\, d\beta$$

$$h_x^{(2)} = -js \int_{-\infty}^{+\infty} \beta [C_1 \exp(\beta z) + C_2 \exp(-\beta z)] \cdot \exp(-j\beta s x)\, d\beta. \quad (7)$$

The arbitrary constants are evaluated in terms of arbitrary constant A_1. The usual boundary conditions are applied; i.e., the b_z's and h_x's should be continuous at all boundaries (interfaces) except that

$$h_x^{\mathrm{YIG}} - H_x^{(1)} = J_y(x) \quad \text{at } z = l. \quad (8)$$

The above condition yields

$$-js \int_{-\infty}^{+\infty} \beta A_1 \frac{F_T(\omega,\beta) \exp\Big\{ j\beta \Big(sp_0 + \sqrt{p_0^2 - n_0^2}\Big) l \Big\} \exp(-j\beta s x)}{\exp\Big(-2j\beta \sqrt{p_0^2 - n_0^2}\, d\Big)} d\beta = J_y(x) \quad (9)$$

where

$$F_T(\omega,\beta) = F_m \exp\Big\{ -2j\beta \sqrt{p_0^2 - n_0^2} \Big\} d \quad (10)$$

and

$$F_m = \Big[\Big(1 + T\exp\Big\{2j\beta\sqrt{p_0^2 - n_0^2}\, d\Big\}\Big) - j\Big[\Big\{ \mu_{33}\Big(sp_0 + \sqrt{p_0^2 - n_0^2}\Big) - s\mu_{31} \Big\} + T\Big\{ \mu_{33}\Big(sp_0 - \sqrt{p_0^2 - n_0^2}\Big) \cdot \exp\Big\{2j\beta\sqrt{p_0^2 - n_0^2} \cdot d\Big\} - s\mu_{31} \Big\} \Big] \coth \beta l \Big]. \quad (11)$$

In (11) T is defined as

$$T = T_r + jT_i \quad (12)$$

where

$$T_r = \frac{-\tanh^2(\beta t) - \big[\mu_{33}^2(p_0^2 - \alpha^2) - 2\mu_{33}p_0\mu_{31} + (\mu_{31})^2\big]}{\tanh^2(\beta t) + \{\mu_{33}(sp_0 - \alpha) - s\mu_{31}\}^2} \quad (13)$$

and

$$T_i = \frac{-2\mu_{33}\alpha \tanh \beta t}{\tanh^2(\beta t) + \{\mu_{33}(sp_0 - \alpha) - s\mu_{31}\}^2}. \quad (14)$$

Equation (9) is now multiplied by $\exp(j\beta' s x)$ and integrated with respect to x, which gives the value of A_1 as

$$A_1 = \frac{\tilde{J}J(\beta) \exp\Big(-2j\beta\sqrt{p_0^2 - n_0^2}\Big) d}{2\pi s\beta F_T(\omega,\beta) \exp\Big\{ j\beta \Big(sp_0 + \sqrt{p_0^2 - n_0^2}\Big) l \Big\}} \quad (15)$$

where

$$\tilde{J}(\beta) = \int_{-\infty}^{+\infty} J_y(x) \exp(j\beta s x)\, dx. \quad (16)$$

The dispersion relation is obtained by equating $F_T(\omega,\beta)$ to zero, i.e., $F_T(\omega,\beta) = 0$; thus

$$\cot(\beta\alpha d) = \frac{(\mu_{33}\alpha)^2 - \tanh(\beta l)\tanh(\beta t)}{\mu_{33}\alpha[\tanh(\beta l) + \tanh \beta t]} \quad (17)$$

where, for convenience, $\sqrt{p_0^2 - n_0^2} = \alpha$.

For guided volume waves, α is required to be positive; this leads to the frequency of allowed forward volume waves as $\omega_3 > \omega > \omega_2$ and that of backward waves as $\omega_2 > \omega > \omega_1$. Here $\omega_1 = \omega_0$, $\omega_3 = [\omega_0(\omega_0 + \omega_m)]^{1/2}$, and the transition frequency $\omega_2 = [\omega_0(\omega_0 + \omega_m \sin^2\theta)]^{1/2}$. As can be seen, the transition frequency increases with the increase of θ.

Magnetostatic Wave Power

The time-averaged magnetostatic wave Poynting vector has been obtained as

$$\bar{\mathrm{P}}\mathrm{oynt}_{\mathrm{av}} = \frac{1}{2} \text{ Real part of } (\boldsymbol{E} \times \boldsymbol{h}^*). \quad (18)$$

Magnetostatic waves are TE waves which have been assumed to have no field variation in the y direction, i.e., $\partial/\partial y = 0$. Therefore, $E_x = 0$, $E_z = 0$, and $h_y = 0$. Thus the average Poynting vector is rewritten as

$$\bar{\mathrm{P}}\mathrm{oynt}_{\mathrm{av}} = \frac{1}{2} \text{ Real part of } (E_y h_z^*). \quad (19)$$

Now we determine E_y and h_z in all the regions. From $\nabla \times \boldsymbol{E} = -j\omega\boldsymbol{b}$, we find that

$$E_y = \frac{s\omega}{\beta} b_z \quad (20)$$

and

$$h_z^* = \left(\frac{\partial \psi}{\partial z}\right)^* \tag{21}$$

Therefore the time-averaged power flowing per unit width is written as

$$P_{\text{av}} = \tfrac{1}{2} \text{ Real part of } \int (E_y h_z^*)\, dz$$

$$P_{\text{av}} = \tfrac{1}{2} \text{ Real part of } \int \left[\frac{s\omega}{\beta} b_z \cdot \left(\frac{\partial \psi}{\partial z}\right)^*\right] dz. \tag{22}$$

In above equation, $b_z = \mu_0[\mu_{31} h_x + \mu_{33} \partial\psi/\partial z]$, YIG region and $h_x = \partial\psi/\partial x$. For the dielectric region $\mu_{31} = 0$ and $\mu_{33} = 1$.

In (22), P_{av} is determined in different regions of the delay line. First

$$h_x = \frac{\partial \psi}{\partial x} = -js \int_{-\infty}^{+\infty} \beta [B_1 \exp(\beta z) + B_z \exp(-\beta z)] \cdot \exp(-j\beta s x)\, d\beta$$

is evaluated in region (1), i.e., $h_x^{(1)}$. Similarly $h_x^{(2)}$ and h_x^{YIG} are also determined. The integrations are performed following the contour method [8], [11], [14]. Similarly $\partial\psi/\partial x$ is also evaluated for different regions by solving the integral. Finally the total average power (per unit width) flowing in the $s(\pm x)$ direction in the delay line is

$$P_{\text{av}}(\text{total}) = \frac{s\omega\mu_0 |G|^2}{4\beta^2} M \tag{23}$$

$$M = M_1 + M_2 + M_{\text{YIG}}.$$

M_1, M_2 and M_{YIG} are average powers flowing in dielectric (1), or Al_2O_3, in dielectric (2), or GGG, and in the YIG film respectively:

$$M_1 = \left[\mu_{33}^2 (sp_0 + \alpha)^2 - 2s\mu_{33}(sp_0 + \alpha)\mu_{31} + \{2\mu_{33}^2 (p_0^2 - \alpha^2) - 4\mu_{33} p_0 \mu_{31}\}\{T_4 \cos(2\beta\alpha d) - T_i \sin(2\alpha\beta d)\} + |\mu_{31}|^2 \{2\{T_r \cos(2\beta\alpha d) - T_i \sin(2\beta\alpha d)\} + 1\} + \{\mu_{33}^2 (sp_0 - \alpha)^2 - 2s\mu_{33}(sp_0 - \alpha)\mu_{31} + |\mu_{31}|^2\} TT^*\right] \cdot [\coth(\beta l) - \beta l \operatorname{csch}^2 \beta l] \tag{24}$$

$$M_2 = \frac{4\mu_{33}^2 \alpha^2 [\tanh(\beta t) - \beta t \operatorname{sech}^2 \beta t]}{[\tanh^2(\beta t) + \{\mu_{33}(sp_0 - \alpha) - s\mu_{31}\}^2]} \cdot \frac{1}{[\tanh^2(\beta t) + \{\mu_{33}(sp_0 - \alpha) - s\mu_{31}\}^2]} \tag{25}$$

$$M_{\text{YIG}} = (-2\beta)\left[(sp_0 + \alpha) ds \mu_{31} + \mu_{31} T_r p_0 \frac{\sin(2\alpha\beta d)}{\alpha\beta} - T_i p_0 \mu_{31} \frac{(1 - \cos 2\alpha\beta d)}{\alpha\beta} + TT^*(sp_0 - \alpha) d\mu_{31} s - \mu_{33}\left\{(sp_0 + \alpha)^2 d + \frac{(p_o^2 - \alpha^2)}{\alpha\beta}\{T_r \sin(2\alpha\beta d) - T_i(1 - \cos 2\alpha\beta d)\} + TT^*(sp_0 - \alpha)^2 d\right\}\right] \tag{26}$$

$$TT^* = \frac{\tanh^2(\beta t) + \{\mu_{33}(sp_0 + \alpha) - s\mu_{31}\}^2}{\tanh^2(\beta t) + \{\mu_{33}(sp_0 - \alpha) - s\mu_{31}\}^2} \tag{27}$$

$$G(\beta) = \frac{\tilde{J}(\beta) \exp(-j\alpha\beta d)}{F_T'(\omega, \beta)}$$

$$F_T'(\omega, \beta) = \frac{\partial F_T(\omega, \beta)}{\partial \beta} \tag{28}$$

$$F_T'(\omega, \beta) = F_{T_r}' + jF_{T_i}' \tag{29}$$

$$F_{T_r}' = -2\alpha d \sin(2\alpha\beta d) + T_r' + \{\mu_{33}(sp_0 + \alpha) - s\mu_{31}\} \cdot \{-2\alpha d \cos(2\alpha\beta d) \coth(\beta l) + l \operatorname{csch}^2(\beta l) \sin(2\alpha\beta)\} + \{\mu_{33}(sp_0 - \alpha) - s\mu_{31}\} \cdot \{T_i' \coth(\beta l) - T_i l \operatorname{csch}^2(\beta l)\} \tag{30}$$

$$F_{T_i}' = -2\alpha d \cos(2\alpha\beta d) + T_i' + \{\mu_{33}(sp_0 + \alpha) - s\mu_{31}\} \cdot \{2\alpha d \coth(\beta l) \sin(2\alpha\beta d) + l \operatorname{csch}^2(\beta l) \cos(2\alpha\beta d)\} + \{\mu_{33}(sp_0 - \alpha) - s\mu_{31}\} \cdot \{-T_r' \coth(\beta l) + T_r l \operatorname{csch}^2(\beta l)\} \tag{31}$$

$$T' = T_r' + jT_i' \tag{32}$$

$$T_r' = \frac{4\alpha\mu_{33} t \operatorname{sech}^2(\beta t)[-\{\mu_{33}(sp_0 - \alpha) - s\mu_{31}\}\{-\tanh(\beta t) + s\mu_{31}\}]}{[\tanh^2(\beta t) + \{\mu_{33}(sp_0 - \alpha) - s\mu_{31}\}^2]^2} \tag{33}$$

$$T_i' = \frac{2\alpha\mu_{33} t \operatorname{sech}^2(\beta t)[\tanh^2(\beta t) - \{\mu_{33}(sp_0 - \alpha) - s\mu_{33}\}^2]}{[\tanh^2(\beta t) + \{\mu_{33}(sp_0 - \alpha) - s\mu_{31}\}^2]}. \tag{34}$$

The power flow is conveniently expressed in terms of the radiation resistance as Total P_{av} (per unit width) flowing in the s direction $= 1/2 R |I_0|^2$, where R is the radiation resistance to the s propagation wave. Thus

$$R = \frac{2P_{\text{av}}(\text{Total})}{|I_0|^2} = \frac{s\omega\mu_0 |G|^2 M}{2\beta^2 |I_0|^2} \tag{35}$$

or

$$R = \frac{s\omega\mu_0 M |\tilde{J}(\beta)|^2}{2\beta^2 |I_0|^2 |F_T'(\omega, \beta)|^2}$$

$$\tilde{J}(\beta) = \int_{-\infty}^{+\infty} J_y(x) \exp(j\beta s x)\, dx. \tag{36}$$

Uniform current flow in microstrip transducers is assumed. This is a reasonable assumption and has been considered in several papers published in past. $J_y(x) = I_0/b$, I_0 is the magnitude of the microwave current flowing in the y direction, and b is the width of the microstrip.

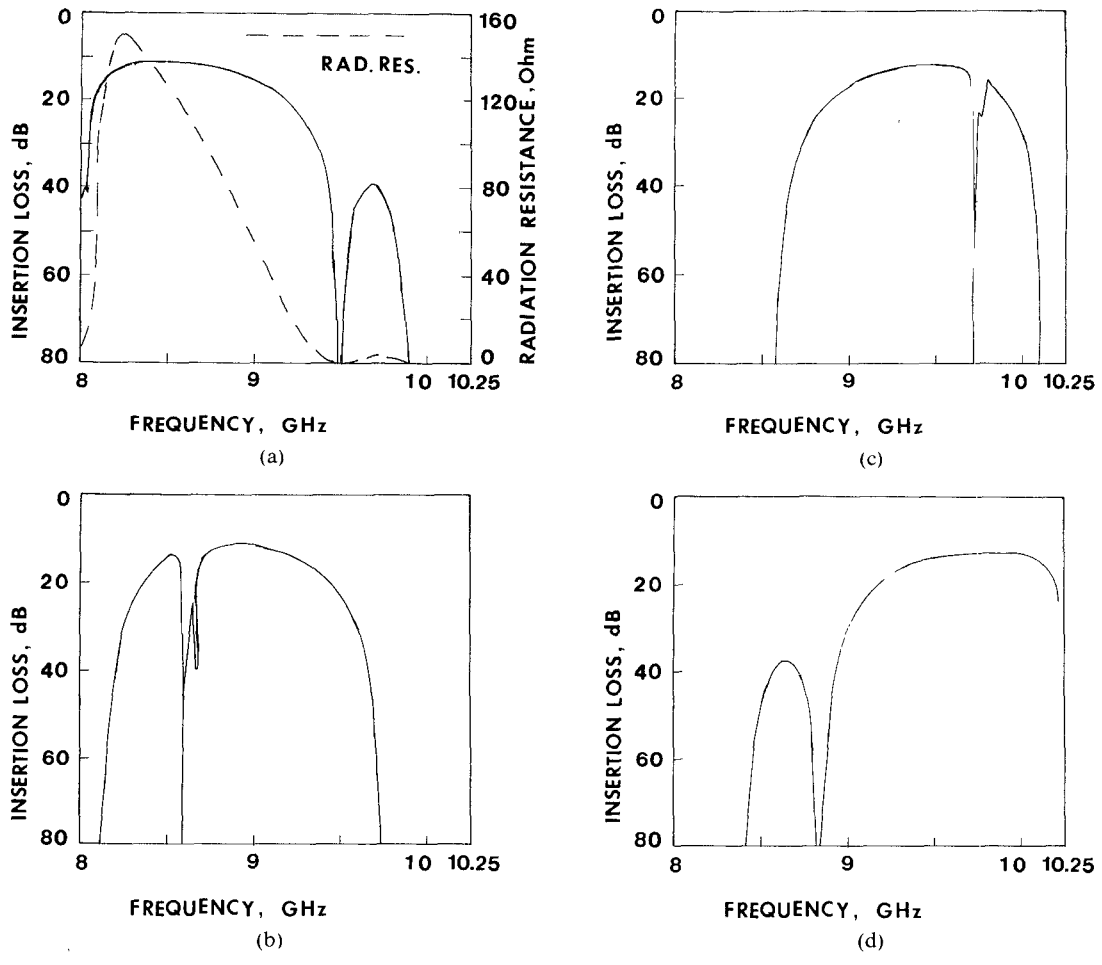

Fig. 2. (a) Variation of insertion loss and radiation resistance with frequency. The parameters are $\theta = 0°$, internal magnetic field $H = 2850$ Oe (corresponding applied magnetic field $H_0 = 4700$ Oe), $d = 50$ μm, $l = 150$ μm, $t = 550$ μm, $b = 50$ μm, width of delay line (W) = 5 mm, $4\pi M_0 = 1850$ gauss, $\gamma = 1.76 \times 10^7$ rad/s·Oe and $\Delta h = 0.5$ Oe. (b) Variation of insertion loss with frequency. Here $\theta = 30°$, transition frequency = 8.60362 GHz; other parameters are the same as in Fig. 2(a). (c) Variation of insertion loss with frequency. Here $\theta = 60°$, transition frequency = 9.7313 GHz; other parameters are the same as in Fig. 2(a). (d) Variation of insertion loss with frequency. Here $\theta = 90°$; other parameters are the same as in Fig. 2(a).

Equation (36) can then be rewritten as

$$\tilde{J}(\beta) = \int_{-b/2}^{+b/2} \frac{I_0}{b} \cdot \exp(j\beta sx)\, dx$$

$$= \frac{I_0}{b} \int_{-b/2}^{+b/2} \exp(j\beta sx)\, dx$$

$$\tilde{J}(\beta) = I_0 s \left[\frac{\sin \beta bs/2}{\beta b/2} \right]$$

$$|\tilde{J}(\beta)|^2 = I_0^2 \left[\frac{\sin \beta b/2}{\beta b/2} \right]^2. \tag{37}$$

Therefore, the radiation resistance (per unit width) for s excitation is rewritten as

$$R = \frac{s\omega\mu_0 M}{2\beta^2 |F_T'(\omega,\beta)|^2} \cdot \left[\frac{\sin \beta b/2}{\beta b/2} \right]^2. \tag{38}$$

The total radiation resistance is obtained as

$$R_{\text{Total}} = |R^+| + |R^-|. \tag{39}$$

In (39), R^+ and R^- are the radiation resistances for $+x$ and $-x$ propagating magnetostatic waves, respectively. Insertion loss ($I.L.$) in the delay line is obtained as

$$I.L. = 20 \log \left[\frac{(R_g + R_{\text{Total}})^2 + (X_{\text{Total}})^2}{4R_g R^+} \right] + \text{Propagation Loss.} \tag{40}$$

In (40), R_g is the source resistance (50 Ω), R_{Total} and X_{Total} are the total radiation resistance and the total radiation reactance of the lowest order mode, respectively, where most of the energy is coupled. X_{Total} is obtained from R_{Total} using the Hilbert transform. R^+ is the radiation resistance of the plus propagating wave in the lowest order mode. Propagation loss was obtained as $76.4 \times \Delta h \times \tau_g$, where Δh is the line width of the YIG film and τ_g is the group delay in microseconds.

As can be clearly seen from (35) and from the terms included in the equation, the entire analysis is very complicated. Expressions obtained in (35) were reduced and compared with expressions obtained by Weinberg and Sethares [15] for specific cases of forward wave (i.e., $\theta = 0$)

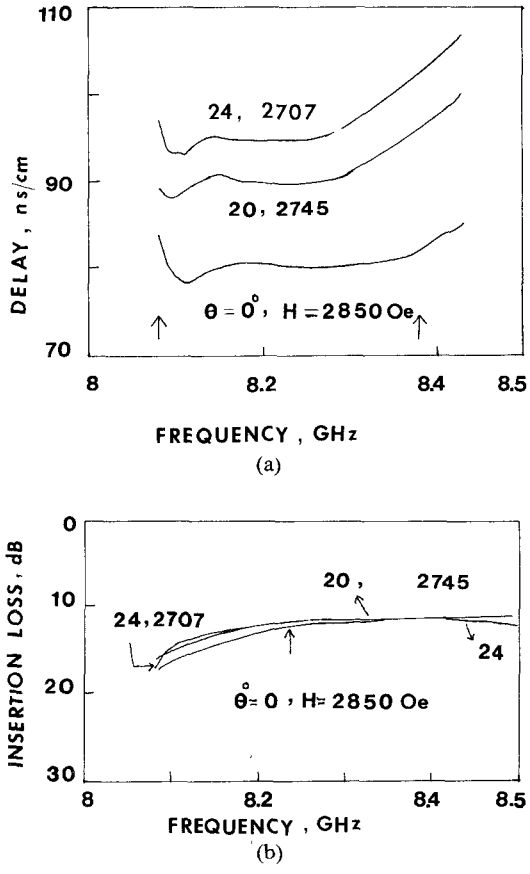

Fig. 3. (a) Variation of constant delays with frequency. Here θ's and H's are shown in the figure; other parameters are the same as in Fig. 2(a). (b) Variation of insertion loss with frequency. Here θ's and H's are shown; other parameters are the same as in Fig. 2(a).

and for full backward wave ($\theta = 90°$) bandwidths, and a complete agreement was seen between our reduced expressions and the expressions obtained by Weinberg and Sethares.

III. Results

In this section variation of insertion loss with frequency is described for various directions of biasing dc magnetic field. Variable constant delay and corresponding insertion loss, as functions of frequency, have been obtained. Finally theoretical and experimental results have been compared and good agreement is seen.

The biasing field (internal magnetic field) is rotated away in the forward volume wave to backward volume wave plane ($Z-X$ plane) in the delay line in Fig. 1. Fig. 2(a) shows the variation of insertion loss with frequency of a magnetostatic wave for $\theta = 0°$. Radiation resistance (or power transduced) for $+x$ and $-x$ excited waves is also shown by the broken line. It can be seen that the insertion loss is minimum where the radiation resistance is maximum. The relationship between insertion loss and radiation resistance for Figs. 2(b)–4 can be similarly understood. Therefore, to avoid crowding, radiation resistance curves in Figs. 2(b)–4 are not drawn. When $\theta = 0°$, the biasing field is normal to the plane of the YIG film. Therefore magnetostatic forward volume waves are excited

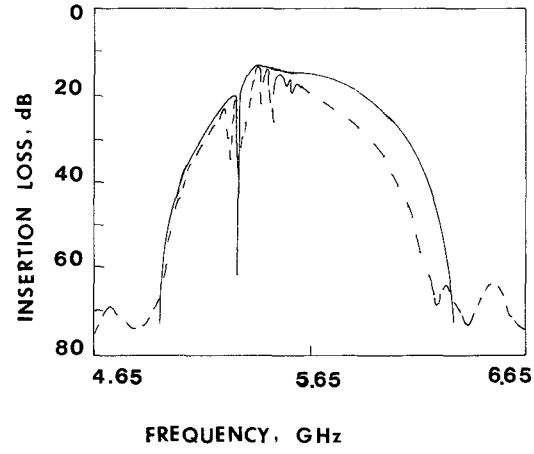

Fig. 4. Variation of insertion loss with frequency: ——— theory; – – – – – experiment. Parameters are $\theta = 28.71°$, internal magnetic field $H = 1704$ Oe (corresponding applied magnetic field $H_0 = 3110$ Oe), $d = 20$ μm, $l = 635$ μm, $t = \infty$, $b = 50$ μm, $W = 5$ mm, $4\pi M_0 = 1750$ Oe, $\gamma = 1.76 \times 10^7$ rad/s·Oe, $\Delta h = 0.9$ Oe, transition frequency = 5.3069 GHz.

in the entire frequency band. As the magnetic field is rotated away from the Z axis in the $Z-X$ plane, the frequency band contains forward as well as backward volume waves in the band (Fig. 2(b) and (c)). The bandwidth of backward volume waves grows at the expense of forward volume waves. When $\theta = 90°$ (Fig. 2(d)) the entire bandwidth contains magnetostatic backward volume waves. The transition from forward volume waves to backward volume waves occurs at a certain frequency, called the transition frequency (F_{Tran}). The transition frequency increases with the rotation of the internal angle of the biasing magnetic field and is shown for each figure.

Fig. 3(a) presents the variation of constant delay with frequency. The first maximum possible bandwidth of constant delay is obtained for the case when the biasing field is normal ($\theta = 0°$) to the YIG film. The bandwidth of constant delay is found to be about 300 MHz. When the biasing field is rotated away from the Z axis, the magnitude of biasing is adjusted (here it is reduced) in order to keep approximately the same bandwidth. It is seen that constant delay times can be varied by adjusting the angle and the magnitude of the biasing magnetic field. The insertion loss variation with frequency for the corresponding bandwidth of variable constant delays (Fig. 3(a)) has been obtained and is shown in Fig. 3(b). It can clearly be seen that insertion loss does not vary in the bandwidth of constant variable delay bandwidth. Near the lower frequency of the bandwidth the insertion loss is slightly higher than at the rest of the frequencies in the band, where constant delays are variable.

Fig. 4 compares theoretical results with our previous measurements [19] for one ground plane. A good agreement between theoretical and experimental results is seen. It is pointed out that the insertion loss curve contains some large ripples around the transition frequency. The exact cause of the large ripples remains unknown; however, sources such as interference between thickness modes of

volume waves, width modes, reflections, and diffractions are thought to contribute to large ripples. So far large ripples have not been found to be completely removed. Efforts by several researchers, however, are being made in this direction.

IV. Summary

An investigation of insertion loss and constant variable delays in electronically variable magnetostatic volume wave delay line has been conducted. The delay line has a conductor–dielectric–YIG–dielectric–conductor structure. Variable delays up to 300 MHz have been obtained in single volume wave delay line by adjusting the direction and the magnitude of the biasing dc magnetic field in the plane containing the normal to the YIG film and the direction of wave propagation. Insertion loss as a function of frequency has been obtained for different biasing field angles and also for the angles corresponding to variable constant delays. A comparison of theoretically obtained insertion loss with experimental results has been made and good agreement is found. Electronically variable magnetostatic wave delay lines hold promise for use in broad-band phased array antennas at 1–20 GHz frequencies.

References

[1] J. M. Owens, R. L. Carter, C. V. Smith, Jr., and J. H. Collins, "Magnetostatic waves, microwave SAW," *Proc. IEEE*, pp. 506–513, 1980.

[2] J. D. Adam and M. R. Daniel, "The status of magnetostatic wave devices," *IEEE Trans. Magn.*, vol. MAG-17, pp. 2951–2956, Nov. 1981.

[3] F. R. Morgenthaler, "MW signal processing with magnetostatic waves and modes," *Microwave J.*, pp. 83–90, Feb. 1982.

[4] J. C. Sethares, "Magnetostatic wave devices and applications," *J. Appl. Phys.*, vol. 53, no. 3, pp. 2646–2651, Mar. 1982.

[5] J. P. Castera, "State of the art in design and technology of MSW devices," *J. Appl. Phys.*, vol. 55, pp. 2506–2511, Mar. 1984.

[6] "Magnetostatic Waves and Applications to Signal Processing," Special Issue of *Circuits, Sys. and Signal Process.*, vol. 4, nos. 1–2, 1985.

[7] S. N. Bajpai, "Magnetostatic waves and devices," *Appl. Phys. Rev.*, to be published.

[8] A. K. Ganguly and D. C. Webb, "Microwave excitation of magnetostatic surface waves: Theory and experiment," *IEEE Trans. Microwave Theory Tech.*, vol. MTT-23, pp. 998–1006, Dec. 1975.

[9] H. J. Wu, C. V. Smith, Jr., J. H. Collins, and J. M. Owens, "Bandpass filtering with multibar magnetostatic surface wave microstrip transducers," *Electron. Lett.*, vol. 13, pp. 610–611, Sept. 29, 1977.

[10] P. R. Emtage, "Interaction of magnetostatic waves with a current," *J. Appl. Phys.*, vol. 49, pp. 4475–4484, Aug. 1978.

[11] J. C. Sethares, "Magnetostatic surface wave transducers," *IEEE Trans. Microwave Theory Tech.*, vol. MTT-27, pp. 902–909, Nov. 1979.

[12] J. P. Parekh and H. S. Tuan, "Meanderline excitation of magnetostatic surface waves," *Proc. IEEE*, vol. 67, pp. 182–183, Jan. 1979.

[13] J. D. Adam and S. N. Bajpai, "Magnetostatic forward volume wave propagation in YIG stripes," *IEEE Trans. Magn.*, vol. MAG-18, pp. 1598–1600, Nov. 1982.

[14] S. N. Bajpai, "Excitation of magnetostatic surface waves: Effect of finite sample width," *J. Appl. Phys.*, vol. 58, no. 2, pp. 910–913, July 15, 1985.

[15] I. J. Weinberg and J. C. Sethares, "Magnetostatic volume waves," in *IEEE MTT-S Int. Microwave Symp. Dig.*, 1983, pp. 253–255.

[16] J. C. Sethares, J. M. Owens, and C. V. Smith, Jr., "MSW Non-dispersive electronically tunable delay elements," *Electron. Lett.*, vol. 16, pp. 825–826, Oct. 1980.

[17] L. R. Adkins *et al.*, "Electronically time delays using cascaded magnetostatic wave delay lines," *J. Appl. Phys.*, vol. 55, pp. 2518–2520, Mar. 1984.

[18] L. R. Adkins *et al.*, "Electronically variable time delays using magnetostatic wave technology," *Microwave J.*, pp. 109–119, Mar. 1986.

[19] S. N. Bajpai, R. W. Weinert, and J. D. Adam. "Variable magnetostatic wave delay lines," *J. Appl. Phys.*, vol. 58, pp. 990–996, July 1985.

[20] S. N. Bajpai, "Magnetostatic variable constant delay line consisting of metal–dielectric–YIG–GGG–metal," *Electron. Lett.*, vol. 20, pp. 783–784, Sept. 1984.

✠

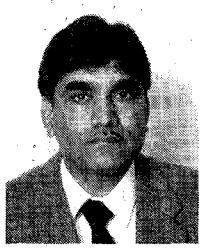

S. N. Bajpai (M'82–SM'84) obtained the Ph.D. degree from the Indian Institute of Technology, Delhi, in 1980.

Since 1983 he has been an Assistant Professor in the Electrical Engineering Department at the State University of New York at Stony Brook, where he teaches graduate and undergraduate courses and conducts microwave research. Prior to joining Stony Brook, he was a visiting Associate Professor (Jan. 83–Aug. 83) in the Electrical Engineering Department at the University of Texas at Arlington, where he was involved in teaching and microwave research. From November 1981 to December 1982 he held the position of Senior Engineer in the Microwave Acoustics and Magnetics section of the Westinghouse Research and Development Center in Pittsburgh, PA. He has taught and performed research in India also.

Dr. Bajpai has been the recipient of a number of scholarships and fellowships. During his stay at Westinghouse he received a Westinghouse Invention Award for his work on "delay control via bias field angle." He was also the recipient of a research grant ("Novel Magnetostatic Wave Devices for 1–20 GHz Applications") awarded by the National Science Foundation. Dr. Bajpai has published more than 20 research papers in various international journals. He is on the editorial board of the IEEE TRANSACTIONS ON MICROWAVE THEORY AND TECHNIQUES. He is a life member of the Indian Association of Physics Teachers. His name is listed in *Who's Who in Frontiers of Science and Technology*. His research interests include microwaves and millimeter waves, electromagnetic theory, magnetics, magneto-optics, fiber optics, microwave optics, and superconductive devices.